Narrow resonances in Rydberg hydrogen spectroscopy

R. G. Bullis, W. L. Tavis, M. R. Weiss, and D. C. Yost
Department of Physics, Colorado State University, Fort Collins, Colorado 80523, USA

(Received 5 July 2024; revised 8 September 2024; accepted 4 November 2024; published 18 November 2024)

We present the recovery of six $2S_{1/2}$-$nS_{1/2}$ two-photon resonances in atomic hydrogen with $8 \leqslant n \leqslant 16$. For each transition, we obtain quality factors $\geqslant 4 \times 10^9$, which we believe are the highest obtained in hydrogen laser spectroscopy excepting the singular $1S_{1/2}$-$2S_{1/2}$ two-photon transition. To the best of our knowledge, the transitions with $n \geqslant 13$ have not been previously observed. These results are enabled by a tightly constrained atomic beam geometry, and by mitigation of the light shift caused by the spectroscopy laser field.

DOI: 10.1103/PhysRevA.110.052807

Owing to its simple atomic structure, spectroscopy of atomic hydrogen has been important in the development of modern physics, and for the determination of fundamental constants [1–15]. In addition, comparisons of hydrogen spectral data with theory can be used as a probe for certain physics beyond the standard model (BSM) [16–26]. Generally, both of these objectives can be pursued simultaneously through the experimental determinations of multiple transitions, which can then be used as input data to global fits [1,23,24,27]. The hydrogen $1S_{1/2}$-$2S_{1/2}$ two-photon transition is notable for its narrow natural linewidth of $\approx$1.4 Hz, and has been measured with an impressive fractional frequency uncertainty of only 4.2×10^{-15} [2]. Unfortunately, all other transitions which are used in global fits have fractional uncertainties at least two orders of magnitude larger. Therefore, an aspirational goal is to measure additional transitions in hydrogen with uncertainties approaching that achieved for the $1S_{1/2}$-$2S_{1/2}$ transition [2].

While not the only consideration, obtaining narrow resonances and correspondingly large quality factors (the transition frequency divided by the resonance width) is highly advantageous in precision measurement. This can be seen from the statistical uncertainty, which is given by

$$\sigma(\tau) \sim \frac{1}{Q\sqrt{N\,\tau}}, \tag{1}$$

where N is the number of atoms measured, τ is the averaging time in seconds, and Q is the quality factor [28]. Therefore, an increase of the transition Q by one order of magnitude equates to two orders of magnitude less averaging time for the same statistical uncertainty. While systematic, and not statistical, uncertainty often limits measurements, many systematic effects are characterized *in situ*, so that the statistical averaging time is still one of the most determinative factors in the overall uncertainty of a measurement. In addition, many systematic effects can produce subtle distortions to the line shape that may be hidden when measuring a broad resonance. For the $1S_{1/2}$-$2S_{1/2}$ transition, the small fractional uncertainty was aided by the recovery of $\approx$2 kHz wide resonances, with a corresponding Q value exceeding 10^{12} [2]. However, there is a notable challenge in obtaining large Q values in hydrogen spectroscopy since the lifetimes of low-lying states other than the $2S_{1/2}$ are comparatively short, which results in broad natural linewidths. The $1S_{1/2}$-$3S_{1/2}$ measurement performed in Garching has a Q value of 2.9×10^9, which was achieved by recovering the natural linewidth (1.0 MHz), and is the second highest in hydrogen laser spectroscopy [13].

With this, spectroscopy of Rydberg levels is attractive since the lifetimes scale as n^3, where n is the principal quantum number [16–19]. In addition, Rydberg levels are much less sensitive to the proton size and quantum electrodynamics corrections, which makes transitions involving Rydberg levels valuable additions to the global hydrogen dataset [29]. Interestingly, the reduced natural linewidth of transitions to Rydberg states has not produced larger Q values than transitions to lower lying states [16–19]. However, the limitations have been technical, and there is opportunity for improvement.

Here, we demonstrate the recovery of narrow resonances for six separate $2S_{1/2}$-$nS_{1/2}$ two-photon transitions with n ranging from 8 to 16. These six transitions were chosen to show the wide applicability of the method, but the method applies to all $2S_{1/2}$-$nS_{1/2}$ transitions in this range. The experimental Q values approach 10^{10} (all exceed 4×10^9) and are the highest reported excepting the $1S_{1/2}$-$2S_{1/2}$ measurement [2]. In addition, to our knowledge, the three shortest wavelength transitions have not been previously observed. These results are enabled by utilizing two-photon Doppler free spectroscopy, tightly constraining the interaction between the atomic beam and laser radiation, and by mitigating the light shift (i.e., the ac Stark shift).

A diagram of our experimental apparatus is shown in Fig. 1 and builds upon the apparatus described in Ref. [30]. A ground state cryogenic hydrogen beam is formed with a cryogenic nozzle ($\sim$5 K) followed by several skimmers to create an atomic beam with a 10 mrad divergence. A portion of this beam is excited to the metastable $2S_{1/2}(F = 1)$ state using cavity enhanced 243 nm radiation with a waist of 150 μm. Next, atoms interact with cavity-enhanced spectroscopy radiation with a beam waist of $\approx$650 μm. The latter cavity is formed using a 5 m radius-of-curvature mirror and a flat mirror, and the cavity finesse is $\approx$2000. The spectroscopy radiation originates from a tunable Ti-sapphire laser, which has a wavelength that varies between 730 and 820 nm depending on the $2S_{1/2}$-$nS_{1/2}$ transition being probed and is directly locked to a stabilized frequency comb referenced to a GPS-disciplined Rb time

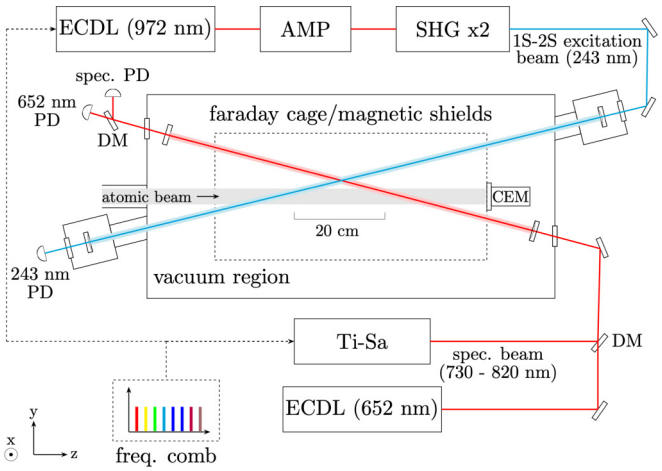

FIG. 1. Experimental apparatus. A cryogenic ground state hydrogen beam interacts with a cavity-enhanced 243 nm radiation source to populate the $2S_{1/2}$ $(F = 1)$ metastable state. This radiation originates from a 972 nm external-cavity diode laser (ECDL) which is amplified and frequency quadrupled using two second harmonic generation (SHG) stages [31]. The atoms then interact with a spectroscopy beam and an ac Stark shift canceling beam (both are enhanced in the same optical cavity) quenching a portion of the $2S_{1/2}(F = 1)$ population. Dichroic mirrors (DM) are used to combine and separate the beams outside of the spectroscopy cavity and photodiodes (PD) are used for cavity locking and power monitoring. The remaining $2S_{1/2}$ atoms are detected with a channel electron multiplier (CEM) to produce the spectroscopic signal.

base (SRS FS740). Typical intracavity spectroscopy power is 60–70 W.

The optical excitation to the metastable state produces a tightly constrained geometry where each $2S_{1/2}$ atom sees a very similar intensity profile as it traverses the spectroscopy laser. If a $2S_{1/2}$-$nS_{1/2}$ transition occurs, the $nS_{1/2}$ state will quickly decay (the lifetimes for $n = 8$ to $n = 16$ upper states are 1–10 μs) with the branching ratios favoring quenching to the ground state. Here, $2S_{1/2}(F = 1)$-$nS_{1/2}(F = 1)$ transitions are probed due to their larger state multiplicity compared to the $2S_{1/2}(F = 0)$-$nS_{1/2}(F = 0)$ transitions. The $2S_{1/2}$ metastable atoms are then detected using a channel-electron multiplier (CEM) and the final detected signal for a $2S_{1/2}$-$nS_{1/2}$ transition manifests as a reduction in metastable counts. This basic experimental setup was used to measure the $2S_{1/2}$-$8D_{5/2}$ transition in Ref. [14]. However, as discussed later, the experimental apparatus now includes an additional laser field at 652 nm which is enhanced in the spectroscopy optical cavity allowing for the approximate cancellation of the ac Stark shift.

While laser cooling has been performed in magnetic traps [32,33] and other methods to produce ultracold hydrogen are being explored [34], these techniques are not yet routine. Therefore, our experiment is performed with an atomic beam, which is the predominant method for hydrogen spectroscopy. With this, one of the most conspicuous challenges to obtaining narrow resonances is the first-order Doppler (FOD) effect. For single-photon transitions, crossed-beam geometries can be used to mitigate the FOD broadening [18,19,35], but it would be extremely challenging to obtain the ∼100 kHz resonances we demonstrate here. The FOD broadening for a single-photon transition is $\Delta v/\lambda$, where Δv is the transverse atomic velocity spread and λ is the wavelength of the spectroscopy beam. In an atomic beam similar to ours, which is highly collimated to a 1 mrad divergence, the transverse velocity is ≈0.4 m/s [30]. For visible wavelengths, this produces broadening on the order of 500 kHz (for a recent example of the progress made in mitigating Doppler broadening in atomic beam experiments, see Ref. [36]).

Therefore, to obtain first-order Doppler free resonances, we measure two-photon $2S_{1/2}$-$nS_{1/2}$ resonances. We focus on S-S transitions because their natural linewidths are narrower than $2S_{1/2}$-nD transitions. The optical cavity which enhances the spectroscopy radiation produces counterpropagating beams that have closely matched wave fronts. Therefore, if an atom absorbs one photon from each direction, the first-order Doppler shifts are equal and opposite [6]. However, there are additional technical challenges besides FOD effects when using this technique. High intensity is required to efficiently drive the transitions, which can produce ∼400 kHz deviations of the line center due to the ac Stark shift [6]. This effect can also broaden the resonance. For example, in Ref. [5], recovered linewidths of the $2S_{1/2}$-$8D_{5/2}$ transition are on the order of 1.3 MHz even though the natural linewidth of the transition is 572 kHz. In that case, the broadening was due to a wide range of atomic trajectories which sampled a correspondingly large range of laser intensities over a 56 cm long interaction region.

In order to mitigate this effect, our apparatus has a tightly constrained geometry. A narrow stripe of metastable $2S_{1/2}$ atoms is produced by the 243 nm radiation which is only ∼150 μm wide (the x direction in Fig. 1). Through this, the metastable beam is collimated in this direction to around 1 mrad and travels ≈20 cm (the z direction in Fig. 1) before interacting with the spectroscopy laser. Therefore, the width of the metastable stripe of atoms is ≈250 μm wide when it interacts with the 650 μm wide spectroscopy radiation and all atoms experience a very similar intensity profile (and corresponding ac Stark shift). As a result, the main effect on the $2S_{1/2}$-$8D_{5/2}$ transition in our apparatus is a simple shift of the line with little additional broadening (recovered linewidths are on the order of 700 kHz [14]).

However, when probing the narrower $2S_{1/2}$-$nS_{1/2}$ transitions, distortions of the line can occur even with this tightly constrained geometry. This is due to the quickly varying ac Stark shift as the atoms pass through the spectroscopy beam's Gaussian spatial profile, along with an atomic coherence time which is long enough to integrate over significant variations in the laser intensity. For example, the $2S_{1/2}$-$12S_{1/2}$ transition has an upper state lifetime of 3.3 μs and, in our apparatus, the interaction time of the atoms with the spectroscopy laser is only ∼20 μs, during which time the atom experiences a rapidly varying laser intensity. The red data points in Fig. 2 show an experimentally recovered line shape for this transition using the experimental apparatus shown in Fig. 1 (without ac Stark shift mitigation). As can be seen, the linewidth is about 350 kHz, and significant line shape distortion occurs. Such distortions due to the ac Stark shift are well understood theoretically [37] and different strategies have been employed to mitigate their effects experimentally [38,39].

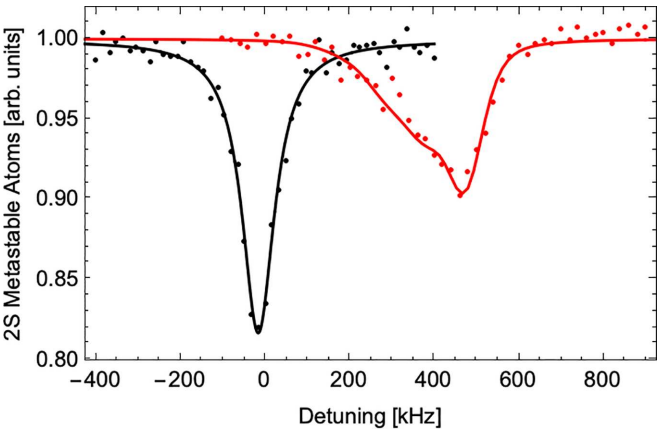

FIG. 2. Experimentally recovered lineshapes for the $2S_{1/2}$-$12S_{1/2}$ transition with ac Stark shift mitigation (black) and without (red). The solid lines are the simulated line shapes obtained by integrating the optical Bloch equations (see text). The approximate spectroscopy and canceling intracavity powers are 70 and 6 W, respectively.

These line distortions are also well represented by our simulations. For this, we use a density matrix model to track the atomic population and coherences as atoms initially in the metastable $2S_{1/2}$ state traverse the spectroscopy beam (for additional details see Supplemental Material of Ref. [14]). For the total signal, we integrate over a reasonable range of trajectories and a modified Maxwellian velocity distribution. The range of spatial trajectories has been determined based on our experimental geometry, and the modified Maxwellian velocity distribution has been determined experimentally [30]. It is important to note that, while our simulation accounts for a spread of atomic trajectories, the basic line shape shown in Fig. 2 is reproduced for a single atomic trajectory.

To counteract these effects, we introduce a secondary radiation field to produce an ac Stark shift nearly equal and opposite to the spectroscopy laser (similar in concept to that shown for rf spectroscopy in [38]). For a given transition, the ac Stark shift coefficients can be analytically calculated [40], and the results for the $2S_{1/2}$-$12S_{1/2}$ transition are shown in Fig. 3. To drive the two-photon transition, light at 750.24 nm

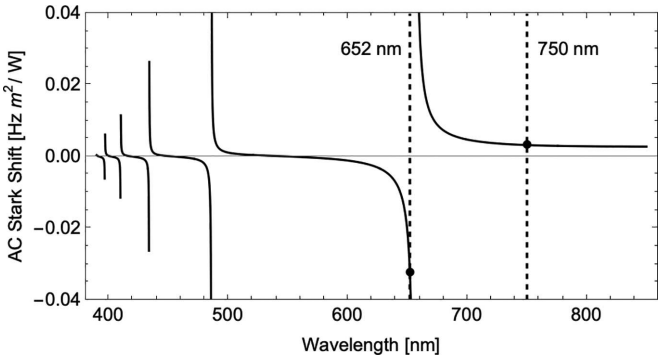

FIG. 3. Analytically calculated ac Stark shift coefficients as a function of laser wavelength for the $2S_{1/2}$-$12S_{1/2}$ transition in atomic hydrogen [40]. The dotted lines show the wavelengths of the spectroscopy laser at 750 nm and the ac Stark shift mitigation laser at 652 nm.

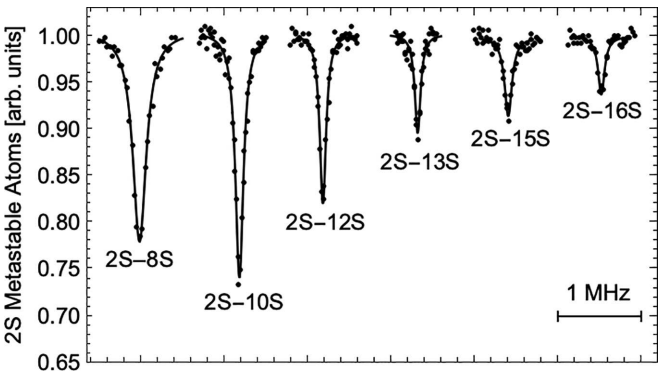

FIG. 4. Recovered resonance spectra for a selection of $2S_{1/2}$-$nS_{1/2}$ two-photon transitions in atomic hydrogen with ac Stark shift mitigation. Spectra are obtained at different spectroscopy laser wavelengths but are plotted adjacent to one another for comparison. The differences in signal size are predominantly due to the variation in the spectroscopy laser power as the wavelength is varied, along with the variation in enhancement cavity mirror reflectivity. With this, the intracavity spectroscopy laser power varied from 60 to 70 W.

is required and, as seen from the figure, the atoms experience a positive ac Stark shift from this laser with a coefficient of 0.0033 Hz m^2/W. To mitigate the ac Stark shift, we introduce radiation at 652 nm which has a coefficient of −0.035 Hz m^2/W.

As shown in Fig. 1, this field is enhanced in the same optical cavity as the spectroscopy beam, and therefore has the same resonant Gaussian beam q-parameter. While this ensures that the two radiation fields are closely overlapped, the beams do not have identical intracavity beam waists. This is because, in vacuum, the waist is given by

$$w = \sqrt{\frac{-\lambda}{\pi\,\mathrm{Im}(1/q)}}. \tag{2}$$

Therefore, the waist for the ac Stark shift compensating radiation is a factor of $\sqrt{652/750} = 0.93$ smaller than that of the spectroscopy laser, and the cancellation of the ac Stark shift cannot be perfect at all positions in the interaction region. Nevertheless, with an appropriate ratio of the two radiation fields, the lines hape distortion can be greatly mitigated. The line shape obtained with 70 W of spectroscopy radiation and with the addition of 6 W of 652 nm radiation is also shown in Fig. 2 along with the simulated line shape showing a drastic reduction in linewidth and distortion.

The spectroscopy laser is sufficiently tunable, and the enhancement cavity mirrors are sufficiently broadband, to address all $2S_{1/2}$-$nS_{1/2}$ transitions with $n \geqslant 6$ ($730 < \lambda < 820$ nm). In addition, these transitions all display a negative ac Stark shift coefficient at 652 nm so that the same experimental techniques can be used to balance the ac Stark shifts for many $2S_{1/2}$-$nS_{1/2}$ transitions. These are shown in Fig. 4 while the extracted linewidths and Q values are shown in Table I. With the cancellation, all transitions are fit with a Lorenztian function in order to extract linewidths and their associated uncertainties through a least-squares fitting routine. As can be seen, all experimentally obtained Q factors exceed 4×10^9,

TABLE I. Transition wavelengths, natural linewidths, experimentally extracted linewidths, and experimentally extracted Q factor for various $2S_{1/2}$-$nS_{1/2}$ two-photon transitions in atomic hydrogen. For reference, we also include $a_{\mathrm{Ry}} = \langle r \rangle$, the effective size of the Rydberg level, in units of the Bohr radius.

	λ (nm)	Γ_{nat} (kHz)	Γ_{exp} (kHz)	Q_{exp} ($\times 10^9$)	a_{Ry} (a_0)
$2S-8S$	778.02	144	195(8)	4.0(2)	96
$2S-10S$	759.79	79	118(4)	6.7(2)	150
$2S-12S$	750.24	48	93(4)	8.6(4)	216
$2S-13S$	747.08	38	84(7)	9.6(8)	254
$2S-15S$	742.60	25	105(8)	7.7(6)	338
$2S-16S$	740.98	21	100(9)	8.1(7)	384

which are the highest obtained in hydrogen laser spectroscopy excepting the $1S_{1/2}$-$2S_{1/2}$ transition. With ac Stark shift mitigation, line-center uncertainties on the order of 200 Hz can be achieved in about 10 minutes of integration for each of the transitions shown. Through simulations and confirmed by experimental observations, we find that intensity variations of the canceling beam by 20% only increases the linewidths by 5%–10% depending on the transition being probed.

The precise measurement of these transitions will require an accurate determination of the residual ac Stark shift by measuring the line centers, as the intensity of both the spectroscopy and 652 nm radiation is varied through a two-dimensional fit, which one might expect would require additional averaging time. However, this depends greatly on the measurement strategy. A conceptually simple approach is to keep the ratio of these two powers constant, so that the true line center is an extrapolation to the point where both powers are zero. This procedure then produces a statistical uncertainty for a given dataset identical to a one-dimensional fit. In practice, it is impossible to keep the powers in exactly the same ratio. However, variations of the ratio by up to 10% have negligible effect on the statistical uncertainty compared to a one-dimensional fit, given our experimentally addressable range of powers.

As is evident from Fig. 2, an additional advantage of the ac Stark shift mitigation is an increase in the signal amplitude. While generally desirable, this property also enables the observation of transitions that would otherwise be very challenging. To our knowledge, the $2S_{1/2}$-$12S_{1/2}$ transition has not been previously studied, due to low signal to noise ratio [6]. In our apparatus, transitions with $n \geqslant 13$ are barely detectable without the mitigation of the ac Stark shift, and, to the best of our knowledge, have not been previously observed.

As shown in Table I, the recovered experimental linewidths are larger than the natural linewidths for all transitions measured. The two most important effects are collisional broadening and transit-time broadening. The collisional broadening is likely the most important effect for the $n = 15$ and $n = 16$ transitions because it scales quadratically with the dipole moment between the nS and nP states (see, for example, Supplemental Material of Ref. [14]). For these transitions, we expect ≈35–45 kHz of broadening at pressures of $\approx 1 \times 10^{-7}$ torr, which could be improved with higher vacuum (for the $2S_{1/2}$-$12S_{1/2}$ transition, we estimate that collisional broadening still contributes about 20 kHz of broadening). Transit-time broadening contributes ∼30 kHz for all transitions. In the near term, a velocity-selective element such as an atomic beam chopper [30] or spectroscopy beam chopper [2] could be used to only perform spectroscopy with atoms of the lowest velocity classes.

While the $2S$ state is sensitive to the proton radius, all of the upper Rydberg levels shown here are relatively insensitive to both QED correction and the proton-radius [29]. Therefore, all transitions are similarly important in determinations of the Rydberg constant.

Nevertheless, there is good motivation for the measurement of several of the transitions shown in Fig. 4. First, many systematic effects, such as the dc Stark shift and collisional shifts, scale rapidly with n. Therefore, the measurement of a collection of levels with increasing upper state n could provide valuable insight into these systematic effects. In addition, some BSM theories [21–23,25,26] introduce light bosons that effectively modify the Coulomb potential over length scales commensurate with the size of a Rydberg atom. The effective size of the upper Rydberg state, given by $a_{\mathrm{Ry}} = \langle r \rangle$, is relevant for these standard model extensions and is also listed for reference in Table I. As shown in the table, we demonstrate that a_{Ry} can be varied by a factor of 4 in a single experimental apparatus, which could provide important information into the scaling of potential BSM physics with n.

To summarize, we have shown the recovery of six resonances involving transitions to Rydberg states in atomic hydrogen. For each transition, we have obtained record high experimental Q values with sufficient signal to noise to obtain line center uncertainties of ∼200 Hz in about 10 minutes of averaging time. The enabling technique for these results was the mitigation of the ac Stark shift through the introduction of an additional radiation field at 652 nm which produces an opposite and nearly equal ac Stark shift to the spectroscopy laser. The recovery of narrow line shapes is robust and does not require perfect cancellation of the ac Stark shift. Finally, we provide a roadmap for how the residual systematic can be characterized in a precision measurement. From this, we expect a significant improvement of the ac Stark shift systematic compared with our previous measurement of the $2S_{1/2}$-$8D_{5/2}$ transition with most smaller systematic effects being similar in magnitude [14].

We would like to thank Jacob Roberts, Sam Brewer, and Christian Sanner for useful conversations and comments on the manuscript. This research was supported by the National Science Foundation (Grant No. PHY–2207298).

[1] E. Tiesinga, P. J. Mohr, D. B. Newell, and B. N. Taylor, CODATA recommended values of the fundamental physical constants: 2018, Rev. Mod. Phys. **93**, 025010 (2021).

[2] C. G. Parthey, A. Matveev, J. Alnis, B. Bernhardt, A. Beyer, R. Holzwarth *et al.*, Improved measurement of the hydrogen $1S-2S$ transition frequency, Phys. Rev. Lett. **107**, 203001 (2011).

[3] F. Nez *et al.*, Precise frequency measurement of the $2S-8S/8D$ transitions in atomic hydrogen: New determination of the Rydberg constant, Phys. Rev. Lett. **69**, 2326 (1992).

[4] M. Weitz *et al.*, Precision measurement of the $1S$ ground-state Lamb shift in atomic hydrogen and deuterium by frequency comparison, Phys. Rev. A **52**, 2664 (1995).

[5] B. de Beauvoir, F. Nez, L. Julien, B. Cagnac, F. Biraben, D. Touahri, L. Hilico, O. Acef, A. Clairon, and J. J. Zondy, Absolute frequency measurement of the $2S-8S/D$ transitions in hydrogen and deuterium: New determination of the Rydberg constant, Phys. Rev. Lett. **78**, 440 (1997).

[6] B. de Beauvoir, C. Schwob, O. Acef, L. Hilico, F. Nez, L. Julien, A. Clairon, and F. Biraben, Metrology of the hydrogen and deuterium atoms: Determination of the Rydberg constant and lamb shifts, Eur. Phys. J. D **12**, 61 (2000).

[7] R. Pohl *et al.*, The size of the proton, Nature (London) **466**, 213 (2010).

[8] A. Antognini *et al.*, Proton structure from the measurement of 2S-2P transition frequencies of muonic hydrogen, Science **339**, 417 (2013).

[9] M. Diermaier, C. B. Jepsen, B. Kolbinger, C. Malbrunot, O. Massiczek, C. Sauerzopf, M. C. Simon, J. Zmeskal, and E. Widmann, In-beam measurement of the hydrogen hyperfine splitting and prospects for antihydrogen spectroscopy, Nat. Commun. **8**, 15749 (2017).

[10] A. Beyer *et al.*, The Rydberg constant and proton size from atomic hydrogen, Science **358**, 79 (2017).

[11] H. Fleurbaey, S. Galtier, S. Thomas, M. Bonnaud, L. Julien, F. Biraben, F. Nez, M. Abgrall, and J. Guena, New measurement of the $1S-3S$ transition frequency hydrogen: Contribution to the proton charge radius puzzle, Phys. Rev. Lett. **120**, 183001 (2018).

[12] N. Bezginov, T. Valdez, M. Horbatsch, A. Marsman, A. C. Vutha, and E. A. Hessels, A measurement of the atomic hydrogen Lamb shift and the proton charge radius, Science **365**, 1007 (2019).

[13] A. Grinin, A. Matveev, D. C. Yost, L. Maisenbacher, V. Wirthl, R. Pohl, T. W. Hänsch, and T. Udem, Two-photon frequency comb spectroscopy of atomic hydrogen, Science **370**, 1061 (2020).

[14] A. D. Brandt, S. F. Cooper, C. Rasor, Z. Burkley, A. Matveev, and D. C. Yost, Measurement of the $2S_{1/2} - 8D_{5/2}$ transition in hydrogen, Phys. Rev. Lett. **128**, 023001 (2022).

[15] R. G. Bullis, C. Rasor, W. L. Tavis, S. A. Johnson, M. R. Weiss, and D. C. Yost, Ramsey spectroscopy of the $2S$ hyperfine interval in atomic hydrogen, Phys. Rev. Lett. **130**, 203001 (2023).

[16] R. Lutwak, J. Holley, P. P. Chang, S. Paine, D. Kleppner and T. Ducas, Circular states of atomic hydrogen, Phys. Rev. A **56**, 1443 (1997).

[17] J. C. De Vries, A precision millimeter-wave measurement of the Rydberg frequency, Ph.D. thesis, Massuchusetts Institute of Technology, 2002.

[18] S. Scheidegger, J. A. Agner, H. Schmutz, and F. Merkt, Metrology of Rydberg states of the hydrogen atom, Phys. Rev. A **108**, 042803 (2023).

[19] S. Scheidegger and F. Merkt, Precision-spectroscopic determination of the binding energy of a two-body quantum system: The hydrogen atom and the proton-size puzzle, Phys. Rev. Lett. **132**, 113001 (2024).

[20] M. S. Safronova, D. Budker, D. DeMille, D. F. J. Kimball, A. Derevianko, and C. W. Clark, Search for new physics with atoms and molecules, Rev. Mod. Phys. **90**, 025008 (2018).

[21] S. G. Karshenboim, Precision physics of simple atoms and constraints on a light boson with ultraweak coupling, Phys. Rev. Lett. **104**, 220406 (2010).

[22] S. G. Karshenboim, Constraints on a long-range spin-independent interaction from precision atomic physics, Phys. Rev. D **82**, 073003 (2010).

[23] M. P. A. Jones, R. M. Potvliege, and M. Spannowsky, Probing new physics using Rydberg states of atomic hydrogen, Phys. Rev. Res. **2**, 013244 (2020).

[24] R. M. Potvliege, A. Nicolson, M. P. A. Jones, and M. Spannowsky, Deuterium spectroscopy for enhanced bounds on physics beyond the standard model, Phys. Rev. A **108**, 052825 (2023).

[25] C. Frugiuele, E. Fuchs, G. Perez, and M. Schlaffer, Constraining new physics models with isotope shift spectroscopy, Phys. Rev. D **96**, 015011 (2017).

[26] J. C. Berengut, D. Budker, C. Delaunay, V. V. Flambaum, C. Frugiuele, E. Fuchs, C. Grojean, R. Harnik, R. Ozeri, G. Perez, and Y. Soreq, Probing new long-range interactions by isotope shift spectroscopy, Phys. Rev. Lett. **120**, 091801 (2018).

[27] D. M. Jacobs, Relativistic Ritz approach to hydrogenlike atoms: Theoretical considerations, Phys. Rev. A **106**, 062810 (2022).

[28] F. Riehle, *Frequency Standards: Basics and Applications* (Wiley VCH, Weinheim, 2004).

[29] U. D. Jentschura and D. C. Yost, Precision Rydberg state spectroscopy with slow electrons and the proton-radius puzzle, Phys. Rev. A **108**, 062822 (2023).

[30] S. F. Cooper, A. D. Brandt, C. Rasor, Z. Burkley, and D. C. Yost, Cryogenic atomic hydrogen beam apparatus with velocity characterization, Rev. Sci. Instrum. **91**, 013201 (2020).

[31] Z. Burkley, A. D. Brandt, C. Rasor, S. F. Cooper, and D. C. Yost, Highly coherent, watt-level deep-UV radiation via a frequency-quadrupled Yb-fiber laser system, Appl. Opt. **58**, 1657 (2019).

[32] I. D. Setija, H. G. C. Werij, O. J. Luiten, M. W. Reynolds, T. W. Hijmans, and J. T. M. Walraven, Optical cooling of atomic hydrogen in a magnetic trap, Phys. Rev. Lett. **70**, 2257 (1993).

[33] C. J. Baker *et al.*, Laser cooling of antihydrogen atoms, Nature (London) **592**, 35 (2021).

[34] S. F. Vazquez-Carson, Q. Sun, J. Dai, D. Mitra, and T. Zelevinsky, Direct laser cooling of calcium monohydride molecules, New J. Phys. **24**, 083006 (2022).

[35] L. Maisenbacher, Precision Spectroscopy of the 2S-nP Transitions in Atomic Hydrogen, Doctoral thesis, Ludwig-Maximilians-Universität München, 2020.

[36] G. Clausen, S. Scheidegger, J. A. Agner, H. Schmutz, and F. Merkt, Imaging-assisted single-photon doppler free laser spectroscopy and the ionization energy of metastable triplet helium, Phys. Rev. Lett. **131**, 103001 (2023).

[37] J. E. Stalnaker, D. Budker, S. J. Freedman, J. S. Guzman, S. M. Rochester, and V. V. Yashchuk, Dynamic stark effect and forbidden-transition spectral line shapes, Phys. Rev. A **73**, 043416 (2006).

[38] A. Kaplan, M. F. Andersen, and N. Davidson, Suppression of inhomogenous broadening in rf spectrosopy of optically trapped atoms, Phys. Rev. A **66**, 045401 (2002).

[39] L. Deng, W. R. Garrett, J. Y. Zhang, and M. G. Payne, Effect of quantum interference on the suppression of the ac Stark shifting of a multiphoton resonance, Phys. Rev. A **52**, 489 (1995).

[40] M. Haas *et al.*, Two-photon excitation dynamics in bound two-body Coulomb systems including ac Stark shift and ionization, Phys. Rev. A **73**, 052501 (2006).